


# Histomorphometric and osteocytic characteristics of cortical bone in male subtrochanteric femoral shaft

Xiaoyu Tong,<sup>1,2</sup>  Markus K. H. Malo,<sup>2</sup> Inari S. Burton,<sup>1,2</sup> Jukka S. Jurvelin,<sup>2,3</sup> Hanna Isaksson<sup>4</sup> and Heikki Kröger<sup>1,5</sup>

<sup>1</sup>*Kuopio Musculoskeletal Research Unit (KMRU), Institute of Clinical Medicine, University of Eastern Finland, Kuopio, Finland*

<sup>2</sup>*Department of Applied Physics, University of Eastern Finland, Kuopio, Finland*

<sup>3</sup>*Diagnostic Imaging Centre, Kuopio University Hospital, Kuopio, Finland*

<sup>4</sup>*Department of Biomedical Engineering, Department of Orthopaedics, Lund University, Lund, Sweden*

<sup>5</sup>*Department of Orthopaedics, Traumatology, and Hand Surgery, Kuopio University Hospital, Kuopio, Finland*

## Abstract

The histomorphometric properties of the subtrochanteric femoral region have rarely been investigated. The aim of this study was to investigate the age-associated variations and regional differences of histomorphometric and osteocytic properties in the cortical bone of the subtrochanteric femoral shaft, and the association between osteocytic and histological cortical bone parameters. Undecalcified histological sections of the subtrochanteric femoral shaft were obtained from cadavers ( $n = 20$ , aged 18–82 years, males). They were cut and stained using modified Masson-Goldner stain. Histomorphometric parameters of cortical bone were analysed with  $\times 50$  and  $\times 100$  magnification after identifying cortical bone boundaries using our previously validated method. Within cortical bone areas, only complete osteons with typical concentric lamellae and cement line were selected and measured. Osteocytic parameters of cortical bone were analyzed under phase contrast microscopy and epifluorescence within microscopic fields ( $0.55 \text{ mm}^2$  for each). The cortical widths of the medial and lateral quadrants were significantly higher than other quadrants ( $P < 0.01$ ). Osteonal area per cortical bone area was lower and cortical porosities were higher in the posterior quadrant than in the other quadrants ( $P < 0.05$ ). Osteocyte lacunar number per cortical bone area was found higher in the young subjects ( $\leq 50$  years) than in the older ones ( $> 50$  years) both before and after adjustments for body height and weight ( $P < 0.05$ ). Moreover, significant but low correlations were found between the cortical bone and osteocytic parameters ( $0.20 \leq R^2 \leq 0.35$ ,  $P < 0.05$ ). It can be concluded that in healthy males, the cortical histomorphometric parameters differ between the anatomical regions of the subtrochanteric femoral shaft, and are correlated with the osteocytic parameters from the same site. These findings may be of use when discussing mechanisms that predispose patients to decreasing bone strength.

**Key words:** bone histomorphometry; cortical bone; osteocyte; regional difference; subtrochanteric femoral shaft.

## Introduction

The weight-bearing skeletal system is continuously subjected to mechanical loading, which affects the morphological and structural features of bone (Cvijanovic et al. 2004). At the proximal femur, histomorphometric studies have mainly focused on the femoral neck (Blain et al. 2008; Thomas et al. 2009). Morphometric characteristics of the

subtrochanteric femoral shaft have been less investigated due to fact that the femoral shaft is stronger than the femoral neck and subtrochanteric fractures occur less frequently than femoral neck or pertrochanteric fractures (Baumgaertner et al. 1995). Previous morphometric studies related to the femoral shaft have focused almost exclusively on the mid-femoral shaft (Thomas et al. 2005; Cooper et al. 2007). However, recently atypical femoral fractures (AFF), often located at the subtrochanteric femoral shaft, have been associated with antiresorptive osteoporotic drugs (Sayed-Noor & Sjoden, 2008; Shane et al. 2014; Misof et al. 2015). According to Tamminen et al. (2013), the low bone formation and changes in bone composition may explain the poor fracture resistance in some AFF patients on long-term bisphosphonate-therapy.

### Correspondence

Xiaoyu Tong, Kuopio Musculoskeletal Research Unit, University of Eastern Finland, POB 1627, FIN-70211 Kuopio, Finland.

T: + 358 417075957; F: + 358 17162940; E: xiaoyu.tong@uef.fi

Accepted for publication 12 June 2017

Article published online 7 August 2017

Also because the intracortical porosity of this location was found to increase with ageing (Zebaze et al. 2010), more studies on subtrochanteric femoral cortex are warranted.

Osteocytes represent approximately 90–95% of all osseous cells in the adult skeleton and they are multi-functional cells (Bonewald, 2007). As former osteoblasts, osteocytes express genes of both the mesenchymal and hemopoietic lineage (Noble, 2008). In response to both mechanical and chemical signals, they are thought to activate osteoblasts and/or osteoclasts to initiate bone remodelling (Milovanovic et al. 2013). Osteocytes also work as regulators of bone mineral homeostasis, e.g. orchestrating exchange of mineral from bone surfaces (Bonewald, 2006; Teti & Zallone, 2009). In the bone structure, osteocytes become individually enveloped in the extracellular matrix within spaces known as lacunae (Johnson, 1966). As osteocytes are potentially difficult to study *in situ* in sufficient quantities, their lacunae are commonly used as substitutes (Carter et al. 2014). Especially in bones undergoing high levels of modelling activity, osteocyte lacunar number may be a close reflection of the number of osteocytes present (Noble et al. 1997). Moreover, the osteocyte density is suggested to reflect the activity of the bone remodelling process (Hernandez et al. 2004), hence the variation in number and viability of the osteocytes may also be linked to bone brittleness and fragility (O'Brien et al. 2004).

In addition, young, healthy bone has been found to present higher preserved osteocyte-lacunar characteristics, in contrast to aged and osteoporotic bone (Kingsmill & Boyde, 1998; Carpentier et al. 2012). Ageing has also been found to diminish the canaliculi per lacuna and interosteon connections, leading to decreased mechanosensitivity of the osteocytes (Milovanovic et al. 2013). Despite long-term negative effects, antiresorptive treatment may improve the vitality of cortical bone osteocytes as well as the number of osteocyte lacunae (Bernhard et al. 2013, Plotkin et al. 2008). On the other hand, as the ability of cortical bone to resist fracture deteriorates with increased age, the age-associated changes of the cortical structure may explain susceptibility to fractures (Chen et al. 2013). In particular, in the human femur, the osteocyte distribution may be associated with age- and anatomical region-dependent cortical microarchitecture. Limited studies on this issue have been published (Frost, 1960; Vashishth et al. 2000; Power et al. 2001, 2002; Busse et al. 2010; Carter et al. 2014). In addition, the understanding of cortical bone changes across adulthood and studies of the underlying morphometric changes that might predispose to subtrochanteric fractures are limited.

The present work aimed to close these gaps by characterizing the complete cross-section of male subtrochanteric femoral shaft with cortical bone histomorphometry and osteocyte analysis. Although AFFs are commonly associated with thickening of the lateral cortex at the fracture site (Koh et al. 2011), whether same regional characteristics exist in normal subjects, remains unknown. We hypothesize

that the histological properties of the lateral cortex at the healthy subtrochanteric femoral shaft will differ from other anatomical quadrants. Our purpose was also to study the association between cortical microarchitectural variation and osteocyte distribution.

## Materials and methods

### Subjects

Proximal femurs were obtained from 20 male cadavers (mean age,  $47 \pm 18.2$  years, range 17–82 years) at Kuopio University Hospital, Kuopio, Finland. The subjects were divided into two sub-groups based on their age: young ( $\leq 50$  years,  $n = 12$ ) and old ( $> 50$  years,  $n = 8$ ; Table 1). There was no previous history of medical conditions or use of drugs known to affect bone metabolism. Ethical approval for collection of samples was granted by the National Authority for Medicolegal Affairs (permission number: 5783/04/044/07).

### Sample preparation

Transverse cross-sections (thickness: 5–10 mm) within the subtrochanteric region ( $\leq 5$  cm below lesser trochanter) of the proximal femur were cut with a band saw (KT-210, Koneteollisuus Oy, Helsinki, Finland). A minor cut was made on the medial bone-edge to act as a control of orientation of the sample during processing and measurements (Fig. 1). Samples were dehydrated in ethanol for at least 48 h before being embedded in polymethylmethacrylate (PMMA) according to standard protocols (Raum, 2008). After embedding, 15- $\mu$ m-thick sections were cut using a microtome

**Table 1** Basic anthropometric data of the cadavers. Individual values and mean  $\pm$  SD are shown.

Age (years)	Group*	Height (cm)	Weight (kg)	BMI (kg m <sup>-2</sup> )
17	1	178	74	23.4
22	1	186	106	30.6
29	1	184	105	31
32	1	171	69	23.6
34	1	187	102	29.2
36	1	177	74	23.6
39	1	185	84	24.5
43	1	171	98	33.5
44	1	179	96	30
46	1	185	85	24.8
48	1	178	85	26.8
50	1	185	108	31.6
52	2	180	136	42
53	2	176	73	23.6
58	2	175	73	23.8
58	2	169	96	33.6
62	2	170	68	23.5
74	2	166	64	23.2
77	2	177	72	23
82	2	165	53	19.5
47 $\pm$ 18.2		177 $\pm$ 6.9	84 $\pm$ 20.4	27.2 $\pm$ 5.3

\*Group 1 ( $\leq 50$  years,  $n = 12$ ); Group 2 ( $> 50$  years,  $n = 8$ ).

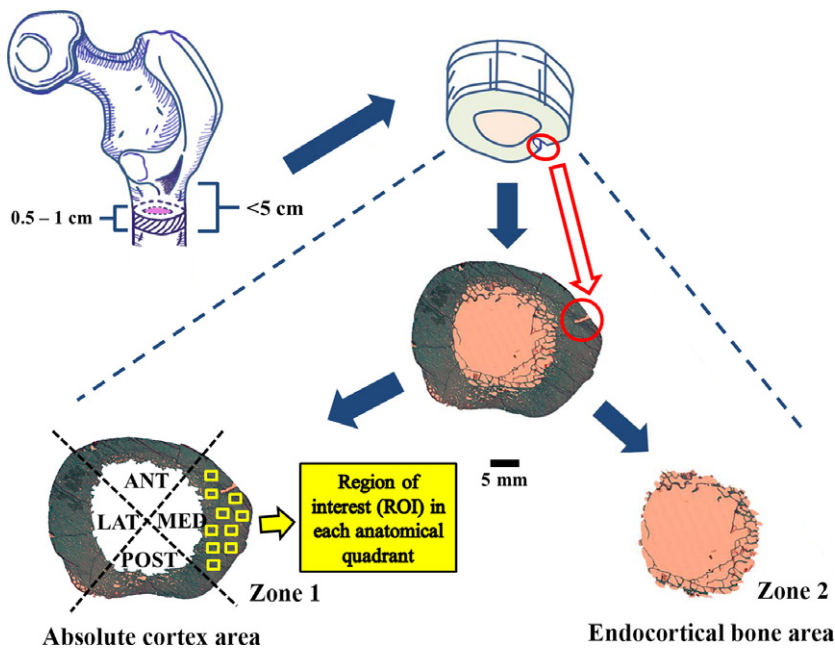


**Fig. 1** Cross-sectional femoral shaft (thickness: 5–10 mm) extracted from the subtrochanteric region (between lesser trochanter and 5 cm distally) of proximal femur were indicated with dashed lines and a minor cut was circled in red on the medial bone edge. The entire cross-sectional femoral shaft was scanned to acquire a complete histological image ( $\times 50$ ), which was separated into two independent zones: the absolute cortex area and the endocortical bone area. The former showed four anatomical quadrants: medial, posterior, lateral and anterior shaft. In each of them, 10 regions of interests (ROI:  $1.51 \text{ mm}^2$  for each) are indicated by solid yellow boxes.

(Reichert-Jung; Cambridge Instruments, Heidelberg, Germany) prior to staining with modified Masson–Goldner trichrome stain. The entire cross-section of the femoral shaft was scanned using an auto-image scanner (Particle Analyzer, Carl Zeiss, Jena, Germany) to acquire a complete histological image ( $\times 50$ ) for histomorphometric analysis. An image program (GNU IMAGE MANIPULATION PROGRAM, version 2.0) was utilized for delineation of different histological boundaries in the images (Tong et al. 2015).

### Cortical bone histomorphometry

Each histological image ( $\times 50$ ) was separated into two independent zones: the absolute cortex area and the endocortical bone area. The former was identified based on the diameter and location of pores, as well as the structural size of the trabeculae, with respect to the 'preliminary cortex boundary'; the latter was identified as the rest of the cross-sectional subtrochanteric femoral shaft (Fig. 1). Full details of the method used to choose the respective area was presented in our earlier study (Tong et al. 2015).

The histomorphometric analyses of cortical bone were conducted using BIOQUANT OSTEO II (Bioquant Image Analysis, Nashville, TN, USA). The nomenclature, abbreviations and parameters follow the recommendations of the American Society for Bone and Mineral Research (ASBMR) (Dempster et al. 2013). First, the samples were analyzed with bright light microscopy using a magnification of  $\times 50$  in images, thereby covering the complete femoral shaft. Then, the absolute cortex area of femoral shaft was divided into four anatomical quadrants (medial, posterior, lateral and anterior; Malo et al. 2013; Fig. 1). After measuring the regional cortical width, the absolute cortex was evaluated under bright light and polarization microscopy using a magnification of  $\times 100$ . For this analysis, in each quadrant, 10 regions of interest (ROI:  $1.51 \text{ mm}^2$  for each) were randomly imaged and measured (Fig. 1). As a result, the  $\times 100$ -magnification parameters were quantified per cortical bone area ( $1.51 \times 10 \times 4 = 60.4 \text{ mm}^2$  for complete sample analysis and  $1.51 \times 10 = 15.1 \text{ mm}^2$  for regional analysis). For osteon analysis, only complete osteons with typical concentric lamellae and cement line were included.

Based on  $\times 50$  magnification imaging, the area and width parameters were determined. Cortical bone area [Ct.Ar. ( $\text{mm}^2$ )] was measured as the area between the absolute cortex boundary and the periosteum. The parameters of cortical bone area per bone area [Ct.Ar/B.Ar. (%)] were also determined. Mean cortical width [Mean Ct.Wi. (mm)] was calculated as the average value of all (average 315 measurements/sample) perpendicular widths between the absolute cortex boundary and the periosteum. Similarly, the regional cortical widths at four different anatomical quadrants were measured, i.e. anterior cortical width [Ant Ct.Wi. (mm)], posterior cortical width [Post Ct.Wi. (mm)], medial cortical width [Medial Ct.Wi. (mm)], and lateral cortical width [Lateral Ct.Wi. (mm)]. In addition, the periosteal perimeter [Ps.Pm. (mm)] and endocortical perimeter [Ec.Pm. (mm)] were measured.

Based on  $\times 100$  magnification imaging, the osteonal and cortical pore parameters were determined. The percentage of osteonal area per cortical bone area was calculated [On.Ar/Ct.Ar. (%)]. The mean osteonal perimeter [On.Pm. ( $\mu\text{m}$ )], mean Haversian canal perimeter [H.Pm. ( $\mu\text{m}$ )] and Haversian canal area [H.Ar. ( $\mu\text{m}^2$ )] were determined as the average value of all (average 90 osteons/quadrant) measured osteonal units. The osteon number per cortical bone area [N.On/Ct.Ar. ( $\#/ \text{mm}^2$ )], the minimum osteonal diameter [Min.On.Dm. ( $\mu\text{m}$ )], and the maximum osteonal diameter [Max-On.Dm. ( $\mu\text{m}$ )] were also determined. The mean wall width [W.Wi. ( $\mu\text{m}$ )] of osteons was calculated using all (average 12 measurements/osteon) perpendicular distances between the Haversian canal boundary and the outer edge of the circular osteon. Moreover, cortical pore area comprised both composite and complete Haversian canals (Dempster et al. 2013). The former refers to the canal of composite osteon created by adjacent osteonal clustering and merging (Bell et al. 2000). The latter is the canal of complete osteons which consists of typical concentric lamellae and cement line (Tong et al. 2017). The cortical porosity [Ct.Po (%)] was calculated as the ratio of pore area divided by Ct.Ar. The porosity of composite canals [Ct.Po<sub>1</sub> (%)] was calculated separately in addition to overall cortical porosity [Ct.Po<sub>2</sub> (%)]. The composite canal number per cortical bone area [N.Po/Ct.Ar. ( $\#/ \text{mm}^2$ )] was also determined.

## Osteocyte analysis

In each quadrant, 10 microscopic fields were selected randomly as the region of interest (ROI: 0.55 mm<sup>2</sup> for each), with two separate image types captured for each field. Phase contrast microscopy was used to measure total osteocyte lacunae, and epifluorescence microscopy to quantify osteocyte lacunae containing stained cell nuclei (Power et al. 2001). Images were scale-calibrated (1587 pixels mm<sup>-1</sup>) with IMAGEJ (Version 1.48, National Institutes of Health, USA). Quantification of total number of osteocyte lacunae and osteocyte per cortical bone area (0.55 × 10 × 4 = 22 mm<sup>2</sup> for complete sample analysis and 0.55 × 10 = 5.5 mm<sup>2</sup> for regional analysis) were semi-automatically performed on phase contrast and fluorescent images, respectively (Fig. 2). The related parameters included osteocyte lacunar number per cortical bone area [N.Ot.Lc/Ct.Ar (#/mm<sup>2</sup>)] and osteocyte number per cortical bone area [N.Ot/Ct.Ar (#/mm<sup>2</sup>)]. Accordingly, the proportion of osteocytes remaining in their lacunae [Occupancy (%)] was determined as the ratio of N.Ot. over N.Ot.Lc.

## Correlations between cortical microarchitectural characteristics and osteocytic parameters

The association between the cortical bone parameters and osteocytic parameters was studied at the complete sample level. The related cortical bone parameters included: Ct.Ar/B.Ar, Mean Ct.Wi, Ps.Pm, Ec.Pm, On.Pm, N.On/Ct.Ar, H.Ar, H.Pm, N.Po/Ct.Ar, Ct.Po<sub>1</sub>, Ct.Po<sub>2</sub>.

## Statistical analysis

The Shapiro–Wilk test was used to determine whether the data were normally distributed. Variations of histomorphometric and osteocytic parameters between age groups (young and old) were statistically evaluated by independent *t*-tests. Analysis of covariance (general linear model) was used to adjust for subject height and weight (Petit et al. 2008). As the ×50 magnification data of four anatomical quadrants was normally distributed and sample sizes were equal (*n* = 20/region), one-way analysis of variance (ANOVA) followed by *post hoc* multiple comparison Tukey–HSD tests were used

to identify the regional differences of cortical width. Analyses of histomorphometric parameters and variations of osteocyte parameters between the anatomical quadrants at ×100 magnification were statistically evaluated by the Kruskal–Wallis test followed by multiple comparison Mann–Whitney tests, due to the regional non-normal data distribution. The Bonferroni correction was applied in the multiple comparison cases. In addition, the relationship between cortical bone and osteocytic parameters was assessed by Pearson's correlation coefficient. All analyses were performed using SPSS statistical software (version 21, SPSS, Chicago, IL, USA). *P*-values ≤ 0.05 were considered to be statistically significant.

## Results

### Age association of cortical characteristics

No significant differences in cortical microarchitectural characteristics were found between the two age groups (≤ 50 years and > 50 years) either before or after the adjustment for height and weight (Table 2). Ct.Po<sub>1</sub> and Ct.Po<sub>2</sub> were both positively correlated with age (*P* < 0.05) and no significant correlations were found between age and other cortical parameters.

### Regional differences of cortical properties

The cortical width varied significantly in four anatomical quadrants (*P* < 0.001). The cortical widths in the medial and lateral quadrants were significantly higher than those detected in the anterior and posterior quadrants (*P* < 0.01; Fig. 3). This reflects the difference in strain pattern and strength between quadrants.

Analysis of cortical microstructure in each of the investigated quadrants revealed significant differences between the posterior and other regions. There were no marked differences in cortical parameters between lateral, medial and anterior quadrants (Table 3, Fig. 4).

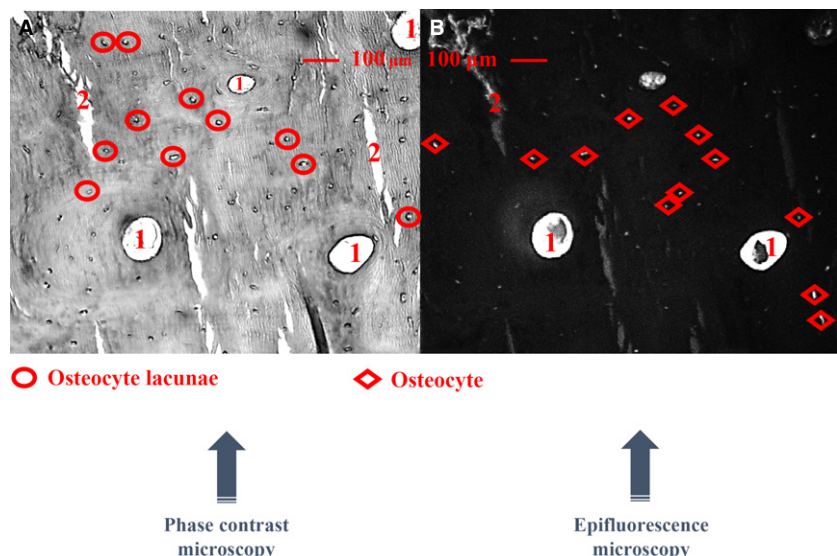


**Fig. 2** Each microscopic field (0.55 mm<sup>2</sup> for each) was selected randomly, capturing two separate image types, phase contrast (A) and fluorescent (B) images, respectively. Quantification of total osteocyte lacunae and osteocytes per cortical bone area were semi-automatically performed. 1: Haversian canals, 2: artificial cracks.



**Table 2** Magnification at  $\times 50$  and  $\times 100$  of cortical bone parameters of the subtrochanteric femoral shaft in two age groups ( $\leq 50$  years,  $> 50$  years). Mean values (standard deviation) are shown.

Parameters	Age $\leq 50$ ( $n = 12$ )	Age $> 50$ ( $n = 8$ )	<i>P</i>	<i>P<sub>H</sub></i>	<i>P<sub>W</sub></i>
$\times 50$ magnification					
Ct.Ar (mm <sup>2</sup> ) <sup>1</sup>	386.6 (52.4)	376.4 (76.0)	0.748	0.254	0.331
Ct.Ar/B.Ar (%) <sup>2</sup>	58.9 (10.1)	55.0 (11.1)	0.435	0.108	0.277
Ps.Pm (mm) <sup>3</sup>	104.2 (7.2)	108.7 (9.9)	0.294	0.660	0.705
Mean Ct.Wi (mm) <sup>4</sup>	5.2 (1.0)	4.8 (1.1)	0.482	0.058	0.254
Ant. Ct.Wi (mm) <sup>5</sup>	4.5 (1.0)	4.5 (0.9)	0.953	0.335	0.690
Post. Ct.Wi (mm) <sup>6</sup>	4.0 (1.1)	3.6 (1.6)	0.536	0.142	0.278
Medial. Ct.Wi (mm) <sup>7</sup>	5.9 (0.9)	5.4 (1.1)	0.383	0.469	0.441
Lateral. Ct.Wi (mm) <sup>8</sup>	5.7 (1.1)	5.5 (0.9)	0.535	0.057	0.061
Ec.Pm (mm) <sup>9</sup>	93.9 (17.9)	105.6 (30.4)	0.347	0.155	0.308
$\times 100$ magnification					
On.Ar/Ct.Ar (%) <sup>10</sup>	14.6 (3.1)	15.2 (3.5)	0.139	0.074	0.112
On.Pm ( $\mu\text{m}$ ) <sup>11</sup>	658.7 (37.3)	663.1 (30.3)	0.973	0.974	0.974
Min.On.Dm ( $\mu\text{m}$ ) <sup>12</sup>	155.5 (8.1)	155.8 (7.6)	0.806	0.989	0.907
Max.On.Dm ( $\mu\text{m}$ ) <sup>13</sup>	201.1 (11.9)	201.8 (8.2)	0.864	0.839	0.855
W.Wi ( $\mu\text{m}$ ) <sup>14</sup>	71.5 (4.1)	70.7 (5.1)	0.526	0.823	0.644
N.On./Ct.Ar (#/mm <sup>2</sup> ) <sup>15</sup>	6.2 (1.2)	6.2 (1.0)	0.749	0.825	0.716
H.Ar ( $\mu\text{m}^2$ ) <sup>16</sup>	1413.4 (209.3)	1514.8 (173.2)	0.254	0.095	0.143
H.Pm ( $\mu\text{m}$ ) <sup>17</sup>	164.8 (12.2)	167.9 (11.2)	0.077	0.058	0.055
N.Po./Ct.Ar (#/mm <sup>2</sup> ) <sup>18</sup>	151.3 (47.4)	186.8 (34.1)	0.236	0.418	0.244
Ct.Po <sub>1</sub> (%) <sup>19</sup>	4.4 (0.7)	5.4 (1.9)	0.087	0.057	0.069
Ct.Po <sub>2</sub> (%) <sup>20</sup>	4.2 (0.7)	5.3 (1.9)	0.079	0.056	0.068

*P* was obtained with an independent *t*-test. *P<sub>H</sub>* and *P<sub>W</sub>* were obtained with a general linear model (univariate procedure) for height and weight adjustments, respectively. <sup>1</sup>Cortical Bone Area (mm<sup>2</sup>). <sup>2</sup>Cortical Bone Area/Bone Area (%). <sup>3</sup>Periosteal Perimeter (mm). <sup>4</sup>Mean Cortical width (mm). <sup>5</sup>Anterior Cortical width (mm). <sup>6</sup>Posterior Cortical width (mm). <sup>7</sup>Medial Cortical width (mm). <sup>8</sup>Lateral Cortical width (mm). <sup>9</sup>Endocortical Perimeter (mm). <sup>10</sup>Osteonal Area/Cortical Bone Area (%). <sup>11</sup>Mean Osteonal Perimeter ( $\mu\text{m}$ ). <sup>12</sup>Min Osteonal Diameter ( $\mu\text{m}$ ). <sup>13</sup>Max Diameter Diameter ( $\mu\text{m}$ ). <sup>14</sup>Mean Wall Width ( $\mu\text{m}$ ). <sup>15</sup>Osteon Number per Cortical Bone Area (#/mm<sup>2</sup>). <sup>16</sup>Haversian canal Area ( $\mu\text{m}^2$ ). <sup>17</sup>Mean Haversian canal Perimeter ( $\mu\text{m}$ ). <sup>18</sup>Pore Number/Cortical Bone Area (#/mm<sup>2</sup>) (complete Haversian canal excluded). <sup>19</sup>Cortical Porosity<sub>1</sub> (%) (complete Haversian canal excluded). <sup>20</sup>Cortical Porosity<sub>2</sub> (%) (complete Haversian canal included).

### Age-association of osteocytic parameters

In complete sample level, each osteocytic parameter were analyzed (Table S1). The N.Ot.Lc/Ct.Ar was higher in the group of young subjects ( $\leq 50$  years) than in the group of old subjects ( $> 50$  years; Fig. 5) both before and after adjustments for body height and weight ( $P < 0.05$ ). The N.Ot.Lc/Ct.Ar was also found to correlate negatively with age ( $P < 0.05$ ). N.Ot/Ct.Ar and Occupancy showed no significant variations between the two age groups and no significant age-association.

### Regional differences of osteocytic parameters

No significant differences in osteocytic parameters were found between the anatomical quadrants (data not shown).

### Relationship between cortical structural characteristics and osteocytic properties

The N.Ot/Ct.Ar and Occupancy were both positively correlated with Ct.Ar/B.Ar and Mean Ct.Wi, but negatively

correlated with Ps.Pm and Ec.Pm ( $0.29 \leq R^2 \leq 0.35$ ,  $P < 0.05$ ). The N.Ot.Lc/Ct.Ar was found to be negatively correlated with Ps.Pm, N.Po/Ct.Ar and both Ct.Po ( $0.20 \leq R^2 \leq 0.29$ ,  $P < 0.05$ ; Table 4).

### Discussion

Although the proximal femur has been studied actively, histomorphometric and osteocytic properties of the subtrochanteric region have rarely been investigated. In the present study, we examined the histological and osteocytic properties of cortical bone structure within complete subtrochanteric femoral shaft cross-sections from healthy male cadavers. The age-associated variations as well as differences between the anatomical regions were determined.

Significant differences in osteon and pore-related parameters between the anatomical quadrants were revealed. This study of normal male cadavers could not find any histomorphometric evidence to explain why the lateral subtrochanteric femoral cortex is most often affected in AFF. However, in most parameters, the posterior region differed from the others. The posterior cortical width was lower

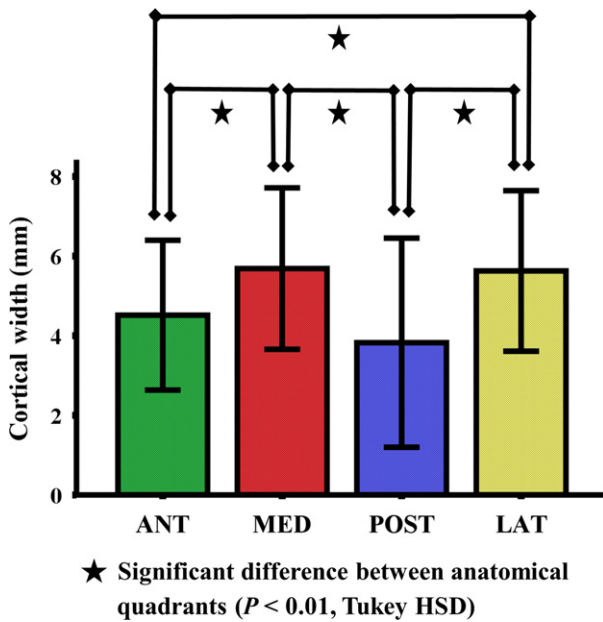


**Fig. 3** Mean values of cortical width in four anatomical quadrants of the subtrochanteric femoral shaft ( $n = 20$ ). The error bars indicate the standard deviation of the mean (SD). The cortical widths in the medial and lateral quadrants were significantly higher than those detected in the anterior and posterior quadrants ( $P < 0.01$ ).

than that of other three quadrants. The thinner cortex may explain the lower osteonal area and osteon number in posterior quadrant compared with the other areas. The cortical pore-related parameters (N.Po/Ct.Ar; both Ct.Po) in the posterior quadrant were higher than those in other quadrants. This is in line with the previous studies (Chen et al. 2010; Chappard et al. 2013) and suggests that the higher porosity

in the posterior quadrant was caused by the increase in both dimension and quantity of the pores. Further, the H.Pm was highest in the posterior quadrant. The expansion of the Haversian canals increases both their perimeter and the cortical porosity (Bell et al. 1999). Therefore, our findings may aid to reveal the underlying morphometric mechanism of higher porosity in the posterior region of subtrochanteric femoral shaft.

At the femoral shaft, an increased periosteal apposition compensates the bone loss caused by the endocortical resorption with age. This effect seems to be least on the posterior surface (Szulc et al. 2006). Minor periosteal apposition may be an indication of low local loading and lower osteon density (Skedros et al. 2001). Toughness of the femoral shaft in tension has also been shown to depend positively on the osteon density (Yeni et al. 1997). In the present study, the lowest osteonal area and density in posterior subtrochanteric femoral shaft cortex provide new evidence for the skeletal remodelling that adjusts the bone structure to meet different load requirements (Mori & Burr, 1993).

The N.Ot.Lc/Ct.Ar was higher in young subjects than in the older ones. This age-associated decline in osteocyte lacunar density is in line with previous studies indicating risks for the structural integrity of bone (Reilly, 2000; Vashishth et al. 2000). Osteocyte density has been suggested to be related to the biomechanical quality of bone (Ma et al. 2008) and also correlates with the initiation and propagation of microdamage (Qiu et al. 2005). Decreased osteocytic number can result in the deterioration of canalicular fluid flow and reduced ability to detect microdamage, leading to increased bone fragility (Burger et al. 2003; Qiu et al. 2003; O'Brien et al. 2004). According to Busse et al.

**Table 3** The median values (standard error) of  $\times 100$  magnification of cortical bone parameters in quadrants of the subtrochanteric femoral shaft.

Parameters	MED	ANT	LAT	POST	H (df)	<i>P</i>
On.Ar/Ct.Ar (%) <sup>1</sup>	15.5 (0.8)	15.3 (0.7)	14.6 (0.8)	12.6 (0.8)*	11.4 (3)	<b>0.01</b>
On.Pm ( $\mu\text{m}$ ) <sup>2</sup>	652.1 (9.3)	667.1 (8.3)	644.0 (9.3)	667.8 (12.0)	2.0 (3)	0.564
Min.On.Dm ( $\mu\text{m}$ ) <sup>3</sup>	153.2 (2.2)	159.2 (2.0)	155.2 (2.0)	157.1 (2.8)	1.9 (3)	0.601
Max.On.Dm ( $\mu\text{m}$ ) <sup>4</sup>	200.0 (2.9)	202.3 (2.5)	195.9 (3.0)	206.0 (3.8)	3.8 (3)	0.285
W.Wi ( $\mu\text{m}$ ) <sup>5</sup>	71.1 (1.1)	72.2 (1.1)	70.4 (1.1)	71.1 (1.4)	0.2 (3)	0.973
N.On/Ct.Ar (#/mm <sup>2</sup> ) <sup>6</sup>	92.5 (3.6)	93.0 (3.8)	99.5 (4.6)	78.0 (4.1)*	13.0 (3)	<b>0.005</b>
H.Ar ( $\mu\text{m}^2$ ) <sup>7</sup>	1340.0 (76.2)	1515.4 (47.8)	1284.2 (55.9)	1638.7 (68.4) <sup>†</sup>	9.8 (3)	<b>0.021</b>
H.Pm ( $\mu\text{m}$ ) <sup>8</sup>	163.1 (4.0)	168.0 (2.9)	158.5 (3.6)	176.9 (4.1) <sup>‡</sup>	10.7 (3)	<b>0.014</b>
N.Po/Ct.Ar (#/mm <sup>2</sup> ) <sup>9</sup>	43.0 (2.9)	37.0 (2.7)	37.0 (2.9)	48.5 (2.3)*	18.9 (3)	<b>&lt;0.05</b>
Ct.Po <sub>1</sub> (%) <sup>10</sup>	2.8 (0.4)	3.0 (0.3)	2.7 (0.6)	5.3 (0.4)*	21.3 (3)	<b>&lt;0.001</b>
Ct.Po <sub>2</sub> (%) <sup>11</sup>	3.9 (0.4)	4.0 (0.3)	3.6 (0.6)	6.1 (0.4)*	20.0 (3)	<b>&lt;0.001</b>

<sup>1</sup>Osteonal Area per Cortical Bone Area (%). <sup>2</sup>Mean Osteonal Perimeter ( $\mu\text{m}$ ). <sup>3</sup>Min Osteonal Diameter ( $\mu\text{m}$ ). <sup>4</sup>Max Diameter Diameter ( $\mu\text{m}$ ). <sup>5</sup>Mean Wall Width ( $\mu\text{m}$ ). <sup>6</sup>Osteon Number per Cortical Bone Area (#/mm<sup>2</sup>). <sup>7</sup>Haversian canal Area ( $\mu\text{m}^2$ ). <sup>8</sup>Mean Haversian canal Perimeter ( $\mu\text{m}$ ). <sup>9</sup>Pore Number per Cortical Bone Area (#/mm<sup>2</sup>) (complete Haversian canal excluded). <sup>10</sup>Cortical Porosity<sub>1</sub> (%) (complete Haversian canal excluded). <sup>11</sup>Cortical Porosity<sub>2</sub> (%) (complete Haversian canal included). *P*-values were obtained with the Kruskal–Wallis test. Significance differences ( $P \leq 0.05$ ) are highlighted in bold. \*Significant difference as compared with the other three quadrants. <sup>†</sup>Significant difference as compared with lateral quadrant. <sup>‡</sup>Significant difference as compared with anterior and lateral quadrants. The *post hoc* multiple comparison was performed with Mann–Whitney tests.

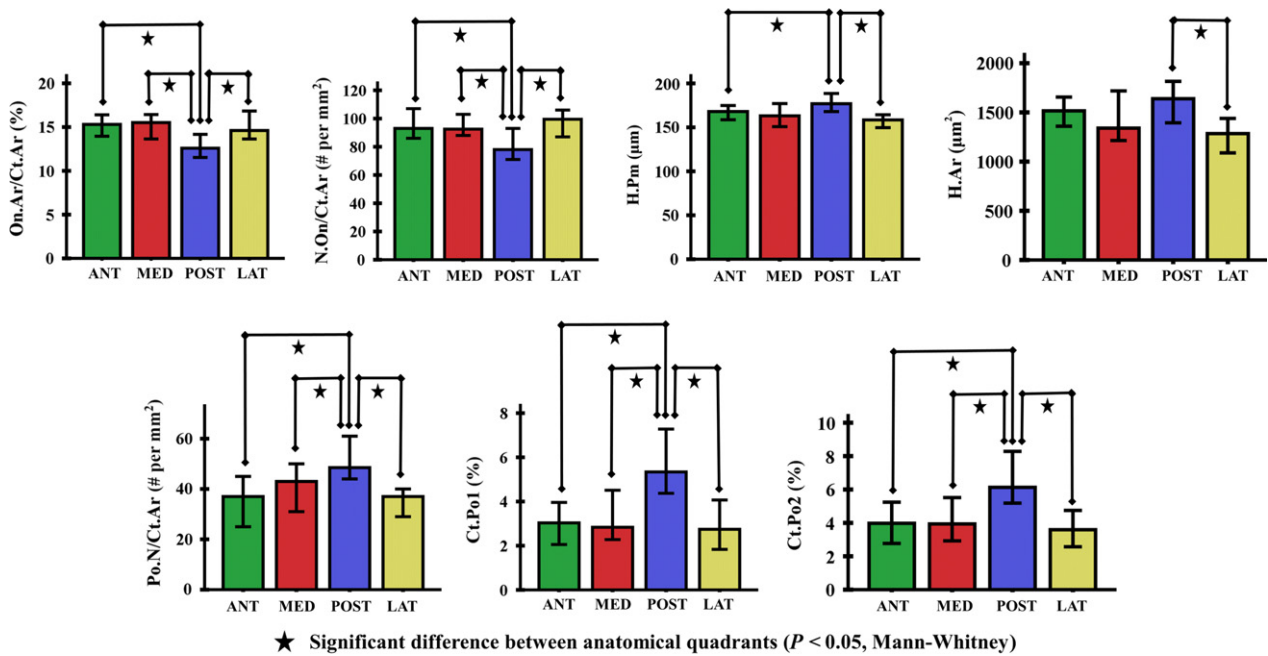


**Fig. 4** The  $\times 100$  magnification cortical parameters of the subtrochanteric femoral shaft showed significant differences in pairwise comparisons between anatomical quadrants ( $P < 0.05$ ). The error bars indicated the standard error of the mean (SEM).

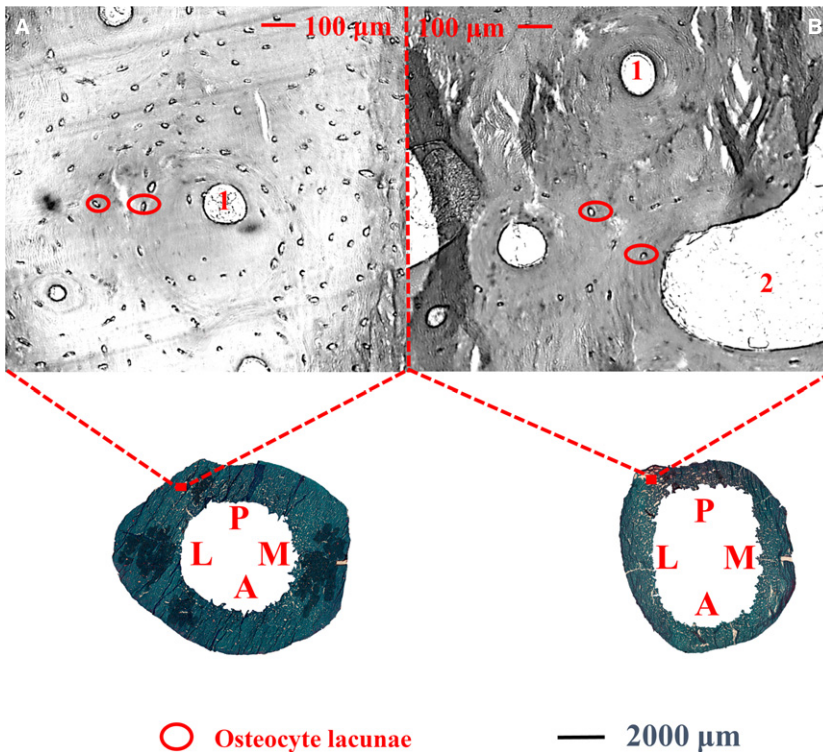


**Fig. 5** Cortex of the subtrochanteric femoral shaft shows the variation of osteocyte lacunar number per cortical bone area in each age group (young: A,  $\leq 50$  years; old: B,  $> 50$  years). Osteocyte lacunae (circled in red) was higher in the group of young subjects (A) than in the group of old subjects (B). 1: Haversian canals, 2: cortical pores. M: medial; P: posterior; L: lateral; A: anterior.

(2010), at the proximal diaphysis, compared with the periosteal region, endocortical bone shows a higher number of hypermineralized lacunae and a lower number of total lacunae. This corresponds with the microarchitectural characteristic that the endocortical surface is affected by more

impaired bone remodelling and much less load than the periosteal surface (Beck et al. 2000; Tanck et al. 2006). Likewise, our finding that N.Ot/Ct.Ar and Occupancy were positively correlated with Ct.Ar/B.Ar and Mean Ct.Wi may also be explained by microarchitectural features. As thicker

**Table 4** Significant correlations between osteocytic parameters and cortical bone parameters of the subtrochanteric femoral shaft.

Parameters	Ct.Ar/B.Ar (%) <sup>1</sup>		Mean Ct. Wi (mm) <sup>2</sup>		Ps.Pm (mm) <sup>3</sup>		Ec.Pm (mm) <sup>4</sup>		N.Po./Ct.Ar (#/mm <sup>2</sup> ) <sup>5</sup>		Ct.Po <sub>1</sub> (%) <sup>6</sup>		Ct.Po <sub>2</sub> (%) <sup>7</sup>	
	<i>r</i>	<i>P</i>	<i>r</i>	<i>P</i>	<i>r</i>	<i>P</i>	<i>r</i>	<i>P</i>	<i>r</i>	<i>P</i>	<i>r</i>	<i>P</i>	<i>r</i>	<i>P</i>
N.Ot.Lc./Ct.Ar (#/mm <sup>2</sup> ) <sup>8</sup>	0.308	0.186	0.215	0.364	-0.483	<b>0.031</b>	-0.411	0.072	-0.508	<b>0.022</b>	-0.45	<b>0.047</b>	-0.485	<b>0.030</b>
N.Ot./Ct.Ar (#/mm <sup>2</sup> ) <sup>9</sup>	0.567	<b>0.009</b>	0.466	<b>0.038</b>	-0.531	<b>0.016</b>	-0.591	<b>0.006</b>	-0.322	0.167	-0.26	0.268	-0.261	0.267
Occupancy (%) <sup>10</sup>	0.542	<b>0.014</b>	0.452	<b>0.046</b>	-0.462	<b>0.041</b>	-0.539	<b>0.014</b>	-0.124	0.603	-0.043	0.857	-0.029	0.904

*P*-values were obtained with Pearson's correlation coefficient. Significance differences ( $P \leq 0.05$ ) are highlighted in bold. <sup>1</sup>Cortical Bone Area per Bone Area (%). <sup>2</sup>Mean Cortical Width (mm). <sup>3</sup>Periosteal Perimeter (mm). <sup>4</sup>Endocortical Perimeter (mm). <sup>5</sup>Pore Number per Cortical Bone Area (#/mm<sup>2</sup>). <sup>6</sup>Cortical Porosity<sub>1</sub> (%) (complete Haversian canal excluded). <sup>7</sup>Cortical Porosity<sub>2</sub> (%) (complete Haversian canal included). <sup>8</sup>Osteocyte Lacunar Number per Cortical Bone Area (#/mm<sup>2</sup>). <sup>9</sup>Osteocyte Number per Cortical Bone Area (#/mm<sup>2</sup>). <sup>10</sup>Occupancy (%).

cortex offers more surfaces on which cortical remodelling may occur, recently formed and rapidly remodelled bone could favour osteocyte survival, leading to higher osteocyte occupancy (Bonewald, 2011).

Moreover, osteocyte apoptosis-induced lacunar hypermineralization with age (Noble, 2003) would potentially weaken the anti-osteoclastogenic function in osteocyte viability, leading to greater cortical porosity (Iwamoto et al. 2010) and increased skeletal fragility (Verborgt et al. 2000). This may explain, at least in part, why the cortical bone porosity accumulates with age, but also indicates the likelihood of an indirect relationship between the osteocyte lacunar density and cortical porosity. In the present study, we found that the N.Ot.Lc./Ct.Ar correlated negatively with the N.Po./Ct.Ar and both Ct.Po. As cortical porosity was increased with age (Bousson et al. 2001) and composite Haversian canals also tended to be found more in the older group, the age-dependent variation of osteocyte lacunar density is consistent with the changes of pore-related cortical parameters during adulthood in the male.

In the present study, there were no significant variations of osteocytic parameters between the anatomical quadrants of the subtrochanteric femoral shaft. This seems inconsistent with the studies carried out by Carter et al., who demonstrated that there was a dramatic difference in osteocyte lacunar density between regions of proximal femora shaft (Carter et al. 2013, 2014). However, unlike the ages of our subjects, spanning the entire male adulthood, all their samples came from relatively young men between the ages of 20 and 35. Therefore, the anatomical region-associated variations may be more characteristic of young bone.

There are some limitations to this study. Firstly, the long-term changes in cortical dimensions and architecture cannot be excluded, as this was a cross-sectional study. Secondly, only male subjects were studied. Thirdly, the moderate number of subjects within each age group means that the power of the study to demonstrate statistically significant differences is comparatively low.

## Conclusion

This study indicates that the cortical histomorphometric parameters differ between the anatomical regions of the subtrochanteric femoral shaft, and are correlated with the osteocytic parameters from the same site. Further studies are needed to investigate whether the variations are related to morphometric changes that might predispose to subtrochanteric fractures.

## Acknowledgements

The authors would like to acknowledge Ms Ritva Sormunen and Dr Arto Koistinen for their assistance in sample preparation and microscopic maintenance. We would also like to acknowledge the financial support from the Sigrid Juselius Foundation, Kuopio University Hospital (VTR 276/2014) and the Strategic Funding of the University of Eastern Finland.

## Conflict of interest

None of the authors has any conflict of interest.

## Author contributions

Study design: T.X.Y., I.B., H.I. and H.K. Data collection: T.X.Y. and M.M. Data analysis: T.X.Y., M.M. and H.K. Data interpretation: T.X.Y., H.I., J.S.J. and H.K. Drafting manuscript: T.X.Y. and I.B. Revising manuscript content: T.X.Y., M.M., I.B., H.I., J.S.J., and H.K. Approving final version of manuscript: T.X.Y., M.M., I.B., H.I., J.S.J. and H.K. T.X.Y. and M.M. take responsibility for the integrity of the data analysis.

## References

- Baumgaertner MR, Curtin SL, Lindskog DM, et al. (1995) The value of the tip-apex distance in predicting failure of fixation of peritrochanteric fractures of the hip. *J Bone Joint Surg Am* 77, 1058-1064.



- Beck TJ, Looker AC, Ruff CB, et al. (2000) Structural trends in the aging femoral neck and proximal shaft: analysis of the Third National Health and Nutrition Examination Survey dual-energy X-ray absorptiometry data. *J Bone Miner Res* **15**, 2297–2304.
- Bell KL, Loveridge N, Power J, et al. (1999) Regional differences in cortical porosity in the fractured femoral neck. *Bone* **24**, 57–64.
- Bell KL, Loveridge N, Jordan GR, et al. (2000) A novel mechanism for induction of increased cortical porosity in cases of intracapsular hip fracture. *Bone* **27**, 297–304.
- Bernhard A, Milovanovic P, Zimmermann EA, et al. (2013) Micro-morphological properties of osteons reveal changes in cortical bone stability during aging, osteoporosis, and bisphosphonate treatment in women. *Osteoporos Int* **24**, 2671–80.
- Blain H, Chavassieux P, Portero-Muzy N, et al. (2008) Cortical and trabecular bone distribution in the femoral neck in osteoporosis and osteoarthritis. *Bone* **43**, 862–868.
- Bonewald LF (2006) Mechanosensation and transduction in osteocytes. *Bonekey Osteovision* **3**, 7–15.
- Bonewald LF (2007) Osteocytes as dynamic multifunctional cells. *Ann N Y Acad Sci* **1116**, 281–290.
- Bonewald LF (2011) The amazing osteocyte. *J Bone Miner Res* **26**, 229–238.
- Bousson V, Meunier A, Bergot C, et al. (2001) Distribution of intracortical porosity in human midfemoral cortex by age and gender. *J Bone Miner Res* **16**, 1308–1317.
- Burger EH, Klein-Nulend J, Smit TH (2003) Strain-derived canalicular fluid flow regulates osteoclast activity in a remodelling osteon – a proposal. *J Biomech* **36**, 1453–1459.
- Busse B, Djonic D, Milovanovic P, et al. (2010) Decrease in the osteocyte lacunar density accompanied by hypermineralized lacunar occlusion reveals failure and delay of remodeling in aged human bone. *Aging Cell* **9**, 1065–1075.
- Carpentier VT, Wong J, Yeap Y, et al. (2012) Increased proportion of hypermineralized osteocyte lacunae in osteoporotic and osteoarthritic human trabecular bone: implications for bone remodeling. *Bone* **50**, 688–694.
- Carter Y, Thomas CD, Clement JG, et al. (2013) Variation in osteocyte lacunar morphology and density in the human femur – a synchrotron radiation micro-CT study. *Bone* **52**, 126–132.
- Carter Y, Suchorab JL, Thomas CD, et al. (2014) Normal variation in cortical osteocyte lacunar parameters in healthy young males. *J Anat* **225**, 328–336.
- Chappard C, Bensalah S, Olivier C., et al. (2013) 3D characterization of pores in the cortical bone of human femur in the elderly at different locations as determined by synchrotron micro-computed tomography images. *Osteoporos Int* **24**, 1023–1033.
- Chen H, Zhou X, Shoumura S, et al. (2010) Age- and gender-dependent changes in three-dimensional microstructure of cortical and trabecular bone at the human femoral neck. *Osteoporos Int* **21**, 627–636.
- Chen H, Zhou X, Fujita H, et al. (2013) Age-related changes in trabecular and cortical bone microstructure. *Int J Endocrinol* **2013**, 213234.
- Cooper DM, Thomas CD, Clement JG, et al. (2007) Age-dependent change in the 3D structure of cortical porosity at the human femoral midshaft. *Bone* **40**, 957–965.
- Cvijanovic O, Bobinac D, Zoricic S, et al. (2004) Age- and region-dependent changes in human lumbar vertebral bone: a histomorphometric study. *Spine* **29**, 2370–2375.
- Dempster DW, Compston JE, Drezner MK, et al. (2013) Standardized nomenclature, symbols, and units for bone histomorphometry: a 2012 update of the report of the ASBMR Histomorphometry Nomenclature Committee. *J Bone Miner Res* **28**, 2–17.
- Frost HM (1960) Micropetrosis. *J Bone Joint Surg* **42-A**, 144–150.
- Hernandez CJ, Majeska RJ, Schaffler MB (2004) Osteocyte density in woven bone. *Bone* **35**, 1095–1099.
- Iwamoto J, Matsumoto H, Takeda T, et al. (2010) Effects of vitamin K2 on cortical and cancellous bone mass, cortical osteocyte and lacunar system, and porosity in sciatic neurectomized rats. *Calcif Tissue Int* **87**, 254–262.
- Johnson LC (1966) The kinetics of skeletal remodeling in structural organization of the skeleton. *Birth Defects* **11**, 66–142.
- Kingsmill VJ, Boyde A (1998) Mineralisation density of human mandibular bone: quantitative backscattered electron image analysis. *J Anat* **192**, 245–256.
- Koh JS, Goh SK, Png MA, et al. (2011) Distribution of atypical fractures and cortical stress lesions in the femur: implications on pathophysiology. *Singapore Med J* **52**, 77–80.
- Ma YL, Dai RC, Sheng ZF, et al. (2008) Quantitative associations between osteocyte density and biomechanics, microcrack and microstructure in OVX rats vertebral trabeculae. *J Biomech* **41**, 1324–1332.
- Malo MK, Rohrbach D, Isaksson H, et al. (2013) Longitudinal elastic properties and porosity of cortical bone tissue vary with age in human proximal femur. *Bone* **53**, 451–458.
- Milovanovic P, Zimmermann EA, Hahn M, et al. (2013) Osteocytic canalicular networks: morphological implications for altered mechanosensitivity. *ACS Nano* **7**, 7542–7551.
- Misof BM, Fratzi-Zelman N, Paschalis EP, et al. (2015) Long-term safety of antiresorptive treatment: bone material, matrix and mineralization aspects. *Bonekey Rep* **4**, 634.
- Mori S, Burr DB (1993) Increased intracortical remodeling following fatigue damage. *Bone* **14**, 103–109.
- Noble BS (2003) Bone microdamage and cell apoptosis. *Eur Cell Mater* **6**, 46–55.
- Noble BS (2008) The osteocyte lineage. *Arch Biochem Biophys* **473**, 106–111.
- Noble BS, Stevens H, Loveridge N, et al. (1997) Identification of apoptotic changes in osteocytes in normal and pathological human bone. *Bone* **20**, 273–282.
- O'Brien CA, Jia D, Plotkin LI, et al. (2004) Glucocorticoids act directly on osteoblasts and osteocytes to induce their apoptosis and reduce bone formation and strength. *Endocrinology* **145**, 1835–1841.
- Petit MA, Beck TJ, Hughes JM, et al. (2008) Proximal femur mechanical adaptation to weight gain in late adolescence: a six-year longitudinal study. *J Bone Miner Res* **23**, 180–188.
- Plotkin LI, Lezcano V, Thostenson J, et al. (2008) Connexin 43 is required for the anti-apoptotic effect of bisphosphonates on osteocytes and osteoblasts *in vivo*. *J Bone Miner Res* **23**, 1712–1721.
- Power J, Noble BS, Loveridge N, et al. (2001) Osteocyte lacunar occupancy in the femoral neck cortex: an association with cortical remodeling in hip fracture cases and controls. *Calcif Tissue Int* **69**, 13–19.
- Power J, Loveridge N, Rushton N, et al. (2002) Osteocyte density in aging subjects is enhanced in bone adjacent to remodeling in avian systems. *Bone* **30**, 859–865.
- Qiu S, Rao DS, Palnitkar S, et al. (2003) Reduced iliac cancellous osteocyte density in patients with osteoporotic vertebral fracture. *J Bone Miner Res* **18**, 1657–1663.
- Qiu S, Rao DS, Fyhrie DP, et al. (2005) The morphological association between microcracks and osteocyte lacunae in human cortical bone. *Bone* **37**, 10–15.

- Raum K** (2008) Microelastic imaging of bone. *IEEE Trans Ultrason Ferroelectr Freq Control* **55**, 1417–1431.
- Reilly GC** (2000) Observations of microdamage around osteocyte lacunae in bone. *J Biomech* **33**, 1131–1134.
- Sayed-Noor AS, Sjoden GO** (2008) Subtrochanteric displaced insufficiency fracture after long-term alendronate therapy – a case report. *Acta Orthop* **79**, 565–567.
- Shane E, Burr D, Abrahamsen B, et al.** (2014) Atypical subtrochanteric and diaphyseal femoral fractures: second report of a task force of the American Society for Bone and Mineral Research. *J Bone Miner Res* **29**, 1–23.
- Skedros JG, Mason MW, Bloebaum RD** (2001) Modeling and remodeling in a developing artiodactyl calcaneus: a model for evaluating Frost's Mechanostat hypothesis and its corollaries. *Anat Rec* **263**, 167–185.
- Szulc P, Seeman E, Duboeuf F, et al.** (2006) Bone fragility: failure of periosteal apposition to compensate for increased endocortical resorption in postmenopausal women. *J Bone Miner Res* **21**, 1856–1863.
- Tamminen IS, Yli-Kyyny T, Isaksson H, et al.** (2013) Incidence and bone biopsy findings of atypical femoral fractures. *J Bone Miner Metab* **31**, 585–594.
- Tanck E, Hannink G, Ruimerman R, et al.** (2006) Cortical bone development under the growth plate is regulated by mechanical load transfer. *J Anat* **208**, 73–79.
- Teti A, Zallone A** (2009) Do osteocytes contribute to bone mineral homeostasis? Osteocytic osteolysis revisited. *Bone* **44**, 11–16.
- Thomas CD, Feik SA, Clement JG** (2005) Regional variation of intracortical porosity in the midshaft of the human femur: age and sex differences. *J Anat* **206**, 115–125.
- Thomas CD, Mayhew PM, Power J, et al.** (2009) Femoral neck trabecular bone: loss with aging and role in preventing fracture. *J Bone Miner Res* **24**, 1808–1818.
- Tong XY, Malo M, Tamminen IS, et al.** (2015) Development of new criteria for cortical bone histomorphometry in femoral neck: intra- and inter-observer reproducibility. *J Bone Miner Metab* **33**, 109–118.
- Tong XY, Burton IS, Isaksson H, et al.** (2017) Iliac crest histomorphometry and skeletal heterogeneity in men. *Bone Rep* **6**, 9–16.
- Vashishth D, Verborgt O, Divine G, et al.** (2000) Decline in osteocyte lacunar density in human cortical bone is associated with accumulation of microcracks with age. *Bone* **26**, 375–380.
- Verborgt O, Gibson GJ, Schaffler MB** (2000) Loss of osteocyte integrity in association with microdamage and bone remodeling after fatigue *in vivo*. *J Bone Miner Res* **15**, 60–67.
- Yeni YN, Brown CU, Wang Z, et al.** (1997) The influence of bone morphology on fracture toughness of the human femur and tibia. *Bone* **21**, 453–459.
- Zebaze RM, Ghasem-Zadeh A, Bohte A, et al.** (2010) Intracortical remodelling and porosity in the distal radius and post-mortem femurs of women: a cross-sectional study. *Lancet* **375**, 1729–1736.

## Supporting Information

Additional Supporting Information may be found in the online version of this article:

**Table S1.** Values of osteocytic parameters in complete sample analysis.